Available online at www.sciencedirect.com
SCIENCE DIRECT
Acta Materialia 54 (2006) 701–711
Acta MATERIALIA
www.actamat-journals.com

A modified embedded-atom method interatomic potential for the Fe–C system

Byeong-Joo Lee *

Department of Materials Science and Engineering, Pohang University of Science and Technology, Hyoja-dong San 31, Pohang 790-784, Republic of Korea

Received 29 April 2005; received in revised form 28 September 2005; accepted 29 September 2005
Available online 22 November 2005

Abstract

A modified embedded-atom method (MEAM) interatomic potential for the Fe–C binary system has been developed using previous MEAM potentials of Fe and C. The potential parameters were determined by fitting to experimental information on the dilute heat of solution of carbon, the vacancy–carbon binding energy and its configuration, the location of interstitial carbon atoms and the migration energy of carbon atoms in body-centered cubic (bcc) Fe, and to a first-principles calculation result for the cohesive energy of a hypothetical NaCl-type FeC. The potential reproduces the known physical properties of carbon as an interstitial solute element in bcc Fe and face-centered cubic Fe very well. The applicability of this potential to atomistic approaches for investigating interactions between carbon interstitial solute atoms and other defects such as vacancies, dislocations and grain boundaries, and also for investigating the effects of carbon on various deformation and mechanical behaviors of iron is demonstrated.

Keywords: Modified embedded-atom method; Iron–carbon alloys; Atomistic simulation; Molecular dynamics; Lattice defect

1. Introduction

Carbon is one of the most important alloying elements in Fe. In addition to the useful effect of carbides on the mechanical properties of steels, with only small additions it has a decisive effect on the deformation behavior and many other properties of steel. Many of the effects of carbon on steel properties originate from strong interactions between interstitial carbon atoms and various defects such as vacancies, self-interstitials, dislocations and grain boundaries.

In order to meet the industrial demand for high-performance steels, it is necessary to ascertain in more detail the effect of individual alloying elements on the properties of steel and to utilize alloying elements more effectively. For this, it is necessary to analyze the stress or strain caused by interstitial carbon atoms or carbides and the interaction between interstitial atoms or carbides and each type of primary defect. All these are atomic-scale problems and can be best investigated using atomistic simulation techniques such as molecular dynamics or Monte Carlo simulations.

First-principles calculations provide the most reliable interatomic potentials for atomistic simulations. However, due to the size (or number of atoms) limit, it is often not possible to investigate material behaviors using only first-principles calculations. Another approach is to use (semi-) empirical interatomic potentials that can deal with more than a million atoms. Important here is that the interatomic potential should be able to reproduce correctly various fundamental physical properties (elastic properties, structural properties, defect properties, surface properties, thermal properties, etc.) of relevant elements or alloys. For this purpose, many (semi-)empirical interatomic potentials have been developed for the Fe–C binary system, by Johnson et al. [1], Rosato [2] and Ruda et al. [3]. The first two investigations paid attention only to the behavior of single interstitial carbon atom in the Fe matrix, and did not consider the carbon–carbon interaction. This is

* Fax: +82 54 279 2399.
E-mail address: calphad@postech.ac.kr.

1359-6454/$30.00
doi:10.1016/j.actamat.2005.09.034

because it was impossible to describe a pure carbon interatomic potential using the potential formalisms used for pure Fe. Without considering the carbon–carbon interaction, these potentials cannot be applied to carbide systems. In the more recent study [3], the authors attempted to include the carbon–carbon interaction based on an embedded-atom formalism [4]. However, with the embedded-atom formalism, which does not consider the angular dependency of binding, the physical properties of pure carbon could not be described well. As a result, the position and migration energy barrier of interstitial carbon atoms in body-centered cubic (bcc) Fe could not be predicted correctly using this potential.

A successful and reliable interatomic potential for an alloy system should be able to reproduce the physical properties of an alloy system over the entire composition range, from one pure element side to the other pure element side, without changing potential parameters or formalism. For this, it is essential to be able to describe individual elements using a common mathematical formalism. Several tens of atomic potential models have been published [5]. Mostly, the models were for a small group of elements. One had to use different formalisms or functional forms for elements of different type (equilibrium structures). This made it difficult to describe alloy systems composed of elements with different structures. From this point of view, the modified embedded-atom method (MEAM [6]) potential may be said to be highly applicable to multi-component systems, because it can describe interatomic potentials of a wide range of elements (face-centered cubic (fcc), bcc, hexagonal close-packed, diamond and even gaseous elements) using a common formalism and functional form. The MEAM was created by Baskes [6], by modifying the embedded-atom method [4,7] to include the directionality of bonding. In the original MEAM [6], interactions among only first-nearest-neighbor atoms were considered. Recently, the MEAM was modified once again by the present author and Baskes (2NN MEAM [8,9]) to consider partially second-nearest-neighbor atom interactions and to remove some critical shortcomings in the original MEAM.

The 2NN MEAM potential formalism has already been applied to develop interatomic potentials for pure bcc [9] and fcc [10] metals. Recently, the formalism was also applied to develop an interatomic potential of pure carbon [11]. Because all these potentials were developed based on the same mathematical formalism, the potentials for individual elements can be easily combined to develop alloy potentials. The purpose of the present work is to develop an interatomic potential for the Fe–C binary system that can describe the physical properties of alloys over the entire composition range, from pure iron to pure carbon, based on the previously developed 2NN MEAM potentials for pure Fe [9] and C [11]. A brief description of the 2NN MEAM formalism for alloy systems, the procedure for the determination of potential parameters to describe the Fe–C system and the calculated fundamental physical properties of Fe–C alloys, especially the interaction of carbon atoms with various point defects (vacancy, foreign or self-interstitial atoms) in bcc and fcc Fe matrices, are presented. Comparisons with available experimental information or other calculation results using different atomic potentials including first-principles calculations are also presented.

2. Interatomic potential

2.1. Potential formalism

In the MEAM, the total energy of a system is given in the following form:

$$E = \sum_i \left[F_i(\bar{\rho}_i) + \frac{1}{2} \sum_{j(\neq i)} \phi_{ij}(R_{ij}) \right], \tag{1}$$

where F_i is the embedding function for an atom i embedded in a background electron density $\bar{\rho}_i$ and $\phi_{ij}(R_{ij})$ is the pair interaction between atoms i and j separated by a distance R_{ij}. For energy calculations, the functional forms for F_i and ϕ_{ij} should be given. The background electron density at each atomic site is computed considering the directionality of bonding, that is, by combining several partial electron density terms for different angular contributions with weight factors $t^{(h)}$ ($h = 1$–3). Each partial electron density is a function of atomic configuration and atomic electron density. The atomic electron densities $\rho^{a(h)}$ ($h = 0$–4) are given as

$$\rho^{a(h)}(R) = \rho_0 \exp[-\beta^{(h)}(R/r_e - 1)], \tag{2}$$

where ρ_0 the atomic electron density scaling factor and $\beta^{(h)}$ the decay lengths are adjustable parameters, and r_e is the nearest-neighbor distance in the equilibrium reference structure. A specific form is given to the embedding function F_i, but not to the pair interaction ϕ_{ij}. Instead, a reference structure where individual atoms are on the exact lattice points is defined and the total energy per atom of the reference structure is estimated from the zero-temperature universal equation of state of Rose et al. [12]. Then, the value of the pair interaction is evaluated from the known values of the total energy per atom and the embedding energy, as a function of the nearest-neighbor distance. In the original MEAM [6], only first nearest-neighbor interactions are considered. The neglect of the second and more distant nearest-neighbor interactions is made effective by the use of a strong many-body screening function [13]. The consideration of the second nearest-neighbor interactions in the modified formalism is effected by adjusting the screening parameters, $C_{\min}$, so that the many-body screening becomes less severe. In addition, a radial cutoff function [13] is applied to reduce calculation time. Details of the MEAM formalism have been published in the literature [6,8–10,13] and will not be repeated here. Only the many-body screening which is the most different part of the MEAM from the other (semi-)empirical potentials is described again in Appendix.

To describe an alloy system, the pair interaction between different elements should be determined. For this, a similar technique that is used to determine the pair interaction for pure elements is applied to binary alloy systems. As for the Fe–C system, a hypothetical Fe_3C $L1_2$ ordered structure is chosen as a reference structure. In the $L1_2$ Fe_3C structure, the total energy per atom (for 3/4 Fe atom + 1/4 C atom) is given as follows:

$$E^{u}_{Fe_3C}(R) = \frac{3}{4}F_{Fe}(\bar{\rho}_{Fe}) + \frac{1}{4}F_{C}(\bar{\rho}_{C}) + \frac{Z_1}{2}\left[\frac{1}{2}\phi_{FeFe}(R) + \frac{1}{2}\phi_{FeC}(R)\right] + \frac{Z_2}{2}\left[\frac{3}{4}S_{Fe}\phi_{FeFe}(aR) + \frac{1}{4}S_{C}\phi_{CC}(aR)\right], \quad (3)$$

where Z_1 and Z_2 are the numbers of first and second nearest-neighbors in the $L1_2$ Fe_3C structure, respectively. In the present case, Z_1 and Z_2 are 12 and 6, respectively. S_{Fe} and S_C are the screening function for the second nearest-neighbor interactions between Fe atoms and between C atoms, respectively, and a is the ratio between the second and first nearest-neighbor distances in the reference structure. The pair interaction between Fe and C can now be obtained in the following form:

$$\phi_{FeC}(R) = \frac{1}{3}E^{u}_{Fe_3C}(R) - \frac{1}{4}F_{Fe}(\bar{\rho}_{Fe}) - \frac{1}{12}F_{C}(\bar{\rho}_{C}) - \phi_{FeFe}(R) - \frac{3}{4}S_{Fe}\phi_{FeFe}(aR) - \frac{1}{4}S_{C}\phi_{CC}(aR). \quad (4)$$

The embedding functions F_{Fe} and F_C can be readily computed. The pair interactions ϕ_{FeFe} and ϕ_{CC} between the same type of atoms can also be computed from the descriptions of individual elements. To obtain $E^{u}_{Fe_3C}(R)$, the universal equation of state [12] should be considered once again for $L1_2$ Fe_3C as follows:

$$E^{u}(R) = -E_c(1 + a^* + da^{*3})e^{-a^*}, \quad (5)$$

where d is an adjustable parameter,

$$a^* = \alpha(R/r_e - 1) \quad (6)$$

and

$$\alpha = \left(\frac{9B\Omega}{E_c}\right)^{1/2}. \quad (7)$$

where r_e is the equilibrium nearest-neighbor distance, E_c is the cohesive energy, B is the bulk modulus and Ω is the equilibrium atomic volume of the reference structure. The parameters E_c, r_e (or Ω), B and d of the $L1_2$ Fe_3C composing the universal equation of state are assumed or determined by experiments or high-level calculations. Then the pair interaction between Fe and C is determined as a function of the interatomic distance R.

2.2. Determination of potential parameters for the Fe–C system

In the present work, the (2NN) MEAM parameters for Fe and C were taken from Lee et al. [9,11] without any modification (see Table 1). As described in the previous section, the extension of the MEAM to alloy systems involves the determination of the pair interaction between different types of atoms. The main work in describing alloy systems using the MEAM is to estimate the potential parameters for the universal equation of state for the reference structure. Eqs. (5)–(7) show that the potential parameters are E_c, r_e (or Ω), B and d. The first three are material properties if the reference structure is a real phase structure that exists on the phase diagram of a relevant system. Experimental data on that phase can be used directly. Otherwise, the parameter values should be optimized so that experimental information for other phases or high-level calculation results can be reproduced, if available, or assumptions should be made. The fourth parameter d is a model parameter. The value can be determined by fitting to the $\partial B/\partial P$ value of the reference structure. When the reference structure is not a real phase, it is difficult to estimate a reasonable value of d for the alloy system. For such alloy systems, d is given an average value of those for pure elements.

In addition to the parameters for the universal equation of state, two more model parameters must be determined to describe the alloy systems. One is the C_{min} value. As can be seen in Table 1, each element has its own value of C_{min}. C_{min} determines the extent of screening of an atom (k) to the interaction between two neighboring atoms (i and j). For pure elements, the three atoms are all the same type (i–k–j = A–A–A or B–B–B). However, in the case of alloys, one of the interacting atoms and/or the screening atom can be different types (there are four cases: i–k–j = A–B–A, B–A–B, A–A–B and A–B–B). Different C_{min} values may have to be given in each case. Another model parameter is the atomic electron density scaling factor ρ_0. For an equilibrium reference structure ($R = r_e$), the values of all atomic electron densities become ρ_0. This is an arbitrary value and does not have any effect on calculations for

Table 1
Set of MEAM potential parameters for pure Fe and C

	E_c	r_e	B	A	$\beta^{(0)}$	$\beta^{(1)}$	$\beta^{(2)}$	$\beta^{(3)}$	$t^{(1)}$	$t^{(2)}$	$t^{(3)}$	C_{max}	C_{min}	d
Fe	4.29	2.48	1.73	0.56	4.15	1.0	1.0	1.0	2.6	1.8	−7.2	2.80	0.36	0.05
C	7.37	1.54	4.45	1.18	4.25	2.8	2.0	5.0	3.2	1.44	−4.48	2.80	1.41	0.00

The units of the cohesive energy E_c, the equilibrium nearest-neighbor distance r_e and bulk modulus B are eV, Å and 10^{12} dyn/cm^2, respectively. The reference structures of Fe and C are bcc and diamond, respectively.

pure elements. This parameter is often omitted when describing the potential model for pure elements. However, for alloy systems, especially for systems where the composing elements have different coordination numbers, the scaling factor (relative difference) has a great effect on calculations.

The nine model parameters discussed above, E_c, r_e, B, d, C_{min} and ρ_0 (there are four binary C_{min} parameters), must be determined to describe the alloy system. The optimization of the model parameters is performed by fitting known physical properties of the alloy system. The experimental physical properties of the Fe–C alloys available in the literature are the dilute heat of solution of carbon [14], the vacancy–carbon binding energy [15–18] and its configuration [19] in bcc Fe, the location of interstitial carbon atoms [20,21] and the migration energy of carbon atoms [18,22,23] in bcc- and fcc Fe. First-principles calculation results are also available for the physical properties of hypothetical NaCl-type FeC [24–26] and for interactions between primary defects and carbon atoms in bcc Fe [27] and fcc Fe [28]. The heat of formation [29] and lattice parameter [30] of the Fe_3C cementite are also valuable experimental information. Finally, it should be remembered that there is no stable carbide phase in the Fe–C binary system (actually, even the cementite is a metastable phase). Therefore, one more empirical criterion considered during the parameter optimization is that no other phase should be predicted as a stable carbide phase in this system.

The parameter values were determined by fitting to the above mentioned experimental or first-principles-calculated physical properties of Fe–C alloys. Individual parameters did not have effects on all the target property values. By investigating which parameter affects which property, an optimized set of parameters could be derived by a systematic trial and error approach. The parameter that has the most significant effect on calculated physical properties was the atomic electron density scaling factor ρ_0. First, it was intended roughly to determine the ratio between ρ_0^C and ρ_0^{Fe}, and the E_c value fitting to the formation energy of NaCl-type FeC and heat of solution of carbon in bcc Fe. The NaCl-type FeC was not stable, and transformed to different structures upon molecular dynamics runs at finite temperatures. The cohesive energy of the resultant transformed structures was often larger than the average of those for pure Fe and carbon, -4.29 and -7.37 eV, respectively, which meant the existence of a stable intermediate phase. Decreasing the stability of these intermediate phases by simply increasing the E_c value yielded too large a heat of solution of carbon in bcc Fe. Therefore, much effort has been made to minimize the stability of these unanticipated structures and to obtain a correct value for the heat of solution of carbon in bcc Fe simultaneously. It was found that to satisfy the above conditions, in addition to the ρ_0 and E_c, some C_{min} parameters (for C–Fe–C and Fe–C–C) had to be adjusted and even the C_{max}(C–Fe–C) parameter had to be given a smaller value than usual. The migration energy of a carbon atom in bcc Fe is defined as the energy difference between an interstitial carbon atom in a tetrahedral site and in an octahedral site. The parameter that has the most significant effect on this property was found to be r_e. Therefore this parameter value was determined by fitting to the experimentally reported migration energy of a carbon atom in bcc Fe. The vacancy–carbon binding energy and its configuration in bcc Fe was mostly affected by C_{min}(Fe–Fe–C) and B, respectively. Therefore, these parameter values could be determined by fitting to the relevant experimental information.

The above procedure was repeated until overall agreements between calculation and the target property values were obtained. The d parameter was given an average value of pure components, because its effect on the overall agreement between calculation and target property values was marginal. Even though more experimental or first-principles calculation data were available for the behavior of carbon atoms in fcc Fe and for cementite, these were not used for parameter optimization but for comparison in order to confirm the transferability of the present MEAM potential, as is shown in the following section. Table 2 shows the final values of the Fe–C alloy parameters and how each was determined.

Here, it should be mentioned that the C_{max} parameters have been given a fixed value of 2.8 [9–11], and have never been counted as adjustable parameters. In the present work, a lower value had to be given to the C_{max}(C–Fe–C) parameter in order to minimize the stability of unanticipated structures and to obtain a correct value for the heat of solution of carbon in bcc Fe simultaneously, as mentioned above. According to the MEAM, C_{min} determines the position of neighboring atoms that completely screens second nearest-neighbor interactions, while C_{max} determines the position of neighboring atoms that begins screening second nearest-neighbor interactions. Low values of C_{min} and C_{max} mean that the second nearest-neighbor interactions are less screened by neighboring first nearest-neighbor atoms. In the NaCl-type FeC structure, for example, all the Fe–Fe interactions and carbon–carbon interactions are second nearest-neighbor interactions. The fact that a lower C_{max} value (1.44) had to be used for the C–Fe–C screening compared to other unary or substitutional alloys (2.80) means that in carbide structures the carbon–carbon interactions may not be screened by nearest-neighbor Fe atoms as much as the second nearest-neighbor interactions in pure carbon. (The second nearest-neighbor interactions in pure carbon are completely screened by nearest-neighbor carbon atoms [11].) The present work shows that C_{max} should also be considered as adjustable parameters, especially for an interstitial solid solution system.

3. Calculation of physical properties

In this section, the fundamental physical properties of the Fe–C alloys calculated using the MEAM potentials shown in Tables 1 and 2 are presented, and compared with experimental information or first-principles calculations.

Table 2
MEAM potential parameters for the Fe–C alloy system and procedure for determining each value

	Selected value	Procedure for determination
E_c	$0.75E_c^{Fe} + 0.25E_c^{C} + 0.95$	Fitting dilute heat of solution of carbon in bcc Fe
r_e	2.364	Fitting migration energy of a carbon atom in bcc Fe
B	2.644	Fitting configuration of vacancy–carbon binding in bcc Fe
d	$0.75d^{Fe} + 0.25d^{C}$	Assumption
C_{min}(Fe–C–Fe)	0.36 $(= C_{min}^{Fe-Fe-Fe})$	Assumption
C_{min}(C–Fe–C)	0.16	Minimizing stability of unanticipated intermediate phases (see text)
C_{min}(Fe–Fe–C)	0.16	Fitting vacancy–carbon binding energy in bcc Fe
C_{min}(Fe–C–C)	0.16	Minimizing stability of unanticipated intermediate phases (see text)
C_{max}(Fe–C–Fe)	2.80	Assumption
C_{max}(C–Fe–C)	1.44	Minimizing stability of unanticipated intermediate phases (see text)
C_{max}(Fe–Fe–C)	2.80	Assumption
C_{max}(Fe–C–C)	2.80	Assumption
ρ_0	$\rho_0^C/\rho_0^{Fe} = 6$	Minimizing stability of unanticipated intermediate phases (see text)

The units of the cohesive energy E_c, the equilibrium nearest-neighbor distance r_e and bulk modulus B are eV, Å and 10^{12} dyn/cm^2, respectively. The reference structure is $L1_2$ Fe_3C.

All calculations were performed allowing full relaxations of individual atoms. The size of the system was 2000 atoms ($10 \times 10 \times 10$ unit cells) for bcc and 864 atoms ($6 \times 6 \times 6$ unit cells) for fcc. It was confirmed that all calculation results were independent of the system size. The 2NN MEAM formalism includes up to second nearest-neighbor interactions. Therefore, the radial cutoff distance during atomistic simulations should be at least larger than the second nearest-neighbor distance in the structures under consideration. All calculations presented here are those performed with a radial cutoff distance whose size is between the second and third nearest-neighbor distances (3.6 Å for bcc and 4.0 Å for other structures). The calculations are independent of the size of the radial cutoff distance if it is larger than the third nearest-neighbor distance. Between the second and third nearest-neighbor distances there is little dependence of the calculation results on the size of the radial cutoff distance. Details can be found in the original descriptions of the Fe MEAM potential [9].

3.1. Carbon in bcc Fe

Table 3 compares interstitial solid solution behaviors of carbon atoms in a bcc Fe matrix calculated using the MEAM potentials with those from experiments or other calculations. The first four quantities are fitted property values, and the others are pure prediction. The MEAM potential gives a very good agreement with experimental data for dilute heat of solution and migration energy of carbon in bcc Fe. As is experimentally accepted [21], for an interstitial carbon atom, the octahedral site is energetically more favorable than the tetrahedral site. Fig. 1 shows the most stable location (octahedral site) of an interstitial carbon atom in bcc Fe. For an interstitial carbon atom in an octahedral site, there are two nearest-neighbor Fe atoms in the ⟨0 0 1⟩ directions and four second nearest-neighbor Fe atoms in the ⟨1 1 0⟩ directions. When compared to pure Fe, the distance between the carbon atom (in the center of the octahedral site) and the nearest Fe atoms increases by 28.7%, while that between the carbon atom and second nearest Fe atoms decreases by −3.8%. According to an earlier empirical potential by Rosato [2] these relaxations are +28.7 and −4.7%, respectively. A recent first-principles calculation [27] gives similar results, +24.3 and −1.8%.

A binding energy between two defects is the energy gained when the two defects are interacting as neighbors to each other compared to when they are separated and non-interacting. Experimental data for the vacancy–carbon binding energy show a large scattering, ranging from 0.41 to 1.1 eV. The lowest value has been taken as the target value in previous studies [1,2] on the development of empirical potentials of the Fe–C system. The first-principles calculation [27] also gives a low value, 0.44 eV. However, in the present study, it was difficult to decrease this value below the current one, 0.9 eV, keeping good agreement with other properties. The present calculation is in better agreement with more recent experimental values, 0.85–1.1 eV [16–18]. It is experimentally reported [19] that in the vacancy–carbon binding the carbon atom is not located on the center of the vacancy, but forms an asymmetric vacancy–carbon pair in the ⟨0 0 1⟩ direction with a distance slightly smaller than half the lattice constant, as shown in Fig. 2. The present calculation, the calculation using the Johnson potential [31] and the first-principles calculation [27] give $0.43a_0$, $0.365a_0$ and $0.4a_0$ (a_0 is the lattice constant) for the distance of the carbon atom from the center of the vacancy, respectively, in qualitative agreement with the experimental information [19].

Two carbon atoms in neighboring octahedral sites can be energetically more stable than those separated without interaction. Fig. 3 shows the configuration of two carbon interstitial atoms with the highest binding energy, 0.34 eV, according to the present potential. The two carbon atoms are arranged along the ⟨1 2 0⟩ direction. A slightly smaller binding energy value (0.32 eV) can be obtained when the two carbon atoms are arranged along the ⟨1 0 0⟩ direction. Similar results have also been obtained for the Johnson potential [1], while the first-principles calculation gives a slightly negative binding energy for the latter case (⟨1 0 0⟩ arrangement, see Table 3). The most stable shape

Table 3
Physical properties of the bcc Fe–C alloys calculated using the present 2NN MEAM potential, in comparison with experimental data or other calculations

In bcc Fe	MEAM expt./calc.	
Dilute heat of solution of carbon (eV)	1.22	1.1 ± 0.2[a]
Migration energy barrier of carbon (eV)	0.82	0.88[b], 0.86[c], 0.81–0.83[d]
Vacancy–carbon binding energy (eV)	0.90	0.41[e], 0.85[f], 1.05[g], 1.1[b]
Vacancy–carbon binding distance (a_0)	0.43	0.41[h], 0.48[i], 0.44[j], 0.365[k], 0.40[j]
Carbon–carbon binding energy (eV)	0.34 ⟨1 2 0⟩ 0.32 ⟨1 0 0⟩	0.08[h], 0.13[j] 0.11[h], −0.09[j]
Self interstitial–carbon binding energy (eV)	0.68	0.56[h], −0.19[j]
Vacancy–two carbon binding energy (eV)	1.86 ⟨1 0 0⟩ 0.49 ⟨1 1 0⟩	1.07[j] 1.50[j]

a_0 is the equilibrium lattice constant and the crystallographic directions ⟨1 2 0⟩, etc., represent the direction of carbon–carbon alignment (see text). The reference states of all bindings are the states where all the individual defects are separated and non-interacting with each other.

[a] Ref. [14].
[b] Ref. [18].
[c] Ref. [22].
[d] Ref. [23].
[e] Ref. [15].
[f] Ref. [17].
[g] Ref. [16].
[h] Empirical potential calculation [1].
[i] Empirical potential calculation [2].
[j] First-principles calculation [27].
[k] Ref. [31].

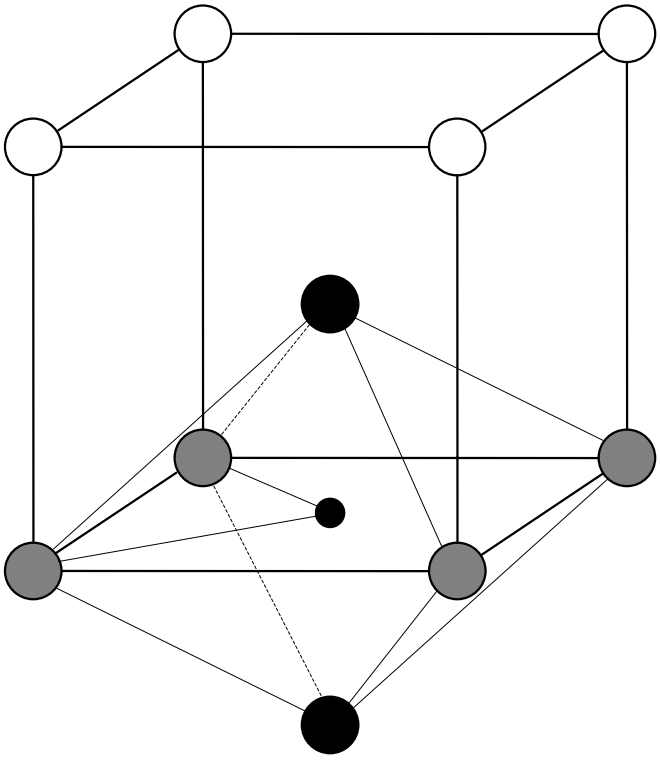

Fig. 1. The most stable configuration of an interstitial carbon atom in an octahedral site of bcc Fe according to the present potential. The small black circle represents the interstitial carbon atom. Large circles represent Fe atoms. The first and second nearest-neighbor Fe atoms to the carbon atom are represented by black and gray circles, respectively.

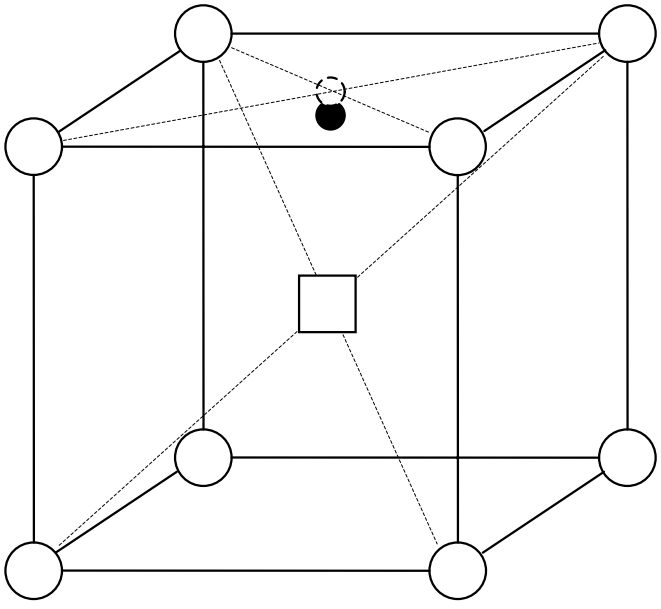

Fig. 2. The most stable configuration of a vacancy–carbon binding in bcc Fe according to the present potential. The small black circle, large white circles and the square represent carbon, Fe atoms and the vacancy, respectively.

of a self-interstitial in bcc Fe is a ⟨1 1 0⟩ dumbbell. The present potential also predicts a strong binding between a self-interstitial and an interstitial carbon atom. There are several interstitial positions for carbon atoms that show

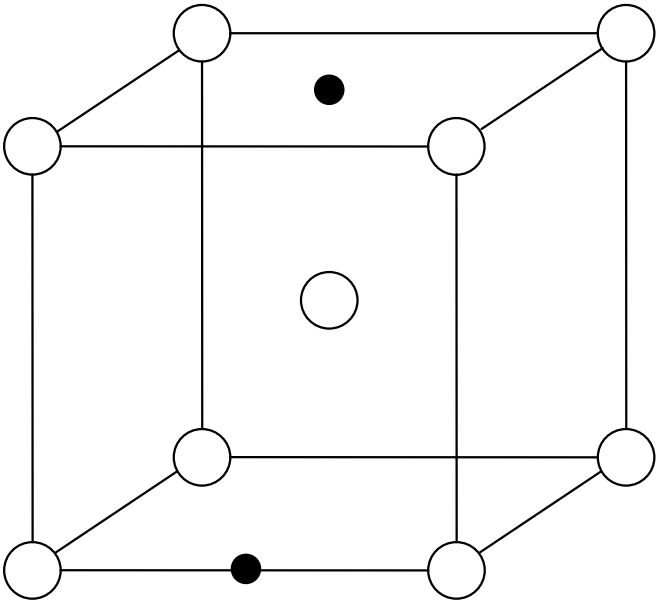

Fig. 3. The most stable configuration of two carbon interstitial atoms in bcc Fe according to the present potential. The small black circles and large white circles represent carbon and Fe atoms, respectively.

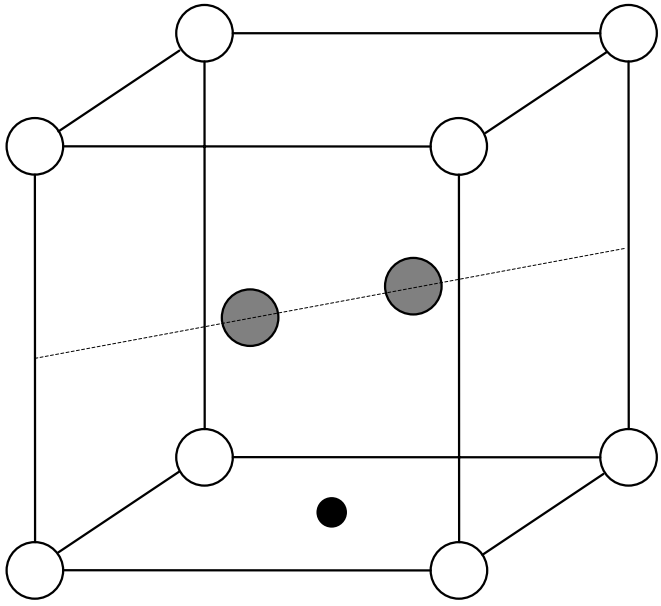

Fig. 4. The most stable configuration of self-interstitial atoms and a carbon interstitial atom in bcc Fe according to the present potential. The small black circle, large white circles and large gray circles represent carbon, normal Fe and self-interstitial Fe atoms, respectively.

positive binding around a self-interstitial. The positions with the largest binding energies are the nearest-neighbor octahedral sites located in the ⟨0 0 1⟩ direction from the center of the ⟨1 1 0⟩ dumbbell, and are shown in Fig. 4. The computed binding energy is 0.68 eV. The stress state for this site should be similar to that of the bottom of an edge dislocation (tensile region), and positive binding with carbon atoms can be easily expected. The earlier potential by Johnson [1] also gives a positive binding energy of 0.56 eV for the same configuration. However, the first-principles calculation [27] predicts a negative binding with a binding energy of −0.39 and −0.19 eV for 54-atom (125 k points) and 128-atom (27 k points) supercells, respectively. The resultant values show a strong dependence on the number of atoms considered, and it seems that a larger number of atoms should be considered to obtain more stable results. According to the present MEAM potential, for example, the dilute heat of solution of carbon in bcc Fe is calculated to be 1.16, 1.19, 1.21, 1.22 and 1.22 eV for system sizes of 54, 128, 251, 432 and 2000, respectively. The calculated defect energies certainly show a size dependency when the system size is smaller than 432 atoms. For binding energy calculations that involve more than two defects, the size dependency would be more severe. The present MEAM calculation proposes that at least 432 atoms should be considered to obtain converged values for single defect formation energy.

Both the present MEAM potential and the first-principles calculation [27] show that binding of a vacancy and two carbon atoms is more stable than a vacancy–carbon pair and a non-interacting carbon interstitial. The binding energy of a vacancy–carbon pair with a second carbon atom is even larger than that of the binding between a vacancy and a carbon atom. However, the two calculations predict the most stable configuration differently. According to the present potential, the most stable vacancy–two carbon binding configuration is to form a ⟨1 0 0⟩ carbon–carbon dumbbell with the vacancy at the center of the dumbbell. This configuration is shown in Fig. 5. It should be mentioned here that actually the carbon atoms are slightly relaxed toward the vacancy, as shown in Fig. 2. The first-principles calculation [27] also predicts a positive binding for this configuration. However, it predicts an even larger binding energy when the two carbon atoms align in the ⟨1 1 0⟩ direction on the nearest-neighbor sites of the vacancy, so that the carbon–vacancy–carbon bonding angle becomes 90°. The present potential predicts that this configuration is more stable than the situation where all the point defects are separated and non-interacting with each other, but less stable than the state where one vacancy–carbon pair is formed and the other carbon atom is non-interacting with this pair.

3.2. Carbon in fcc Fe

The same calculations were performed for the solid solution behavior of carbon in fcc Fe. The results are compared with available experimental data or other calculations in Table 4. These properties were not considered during potential parameter optimization, and therefore the MEAM calculation results in Table 4 are pure predictions. The octahedral vacant site is again the most stable site for interstitial carbon atoms in fcc Fe, and the dilute heat of solution of carbon is calculated to be 0.3 eV. A recently reported first-principles calculation [28] gives a lower value of

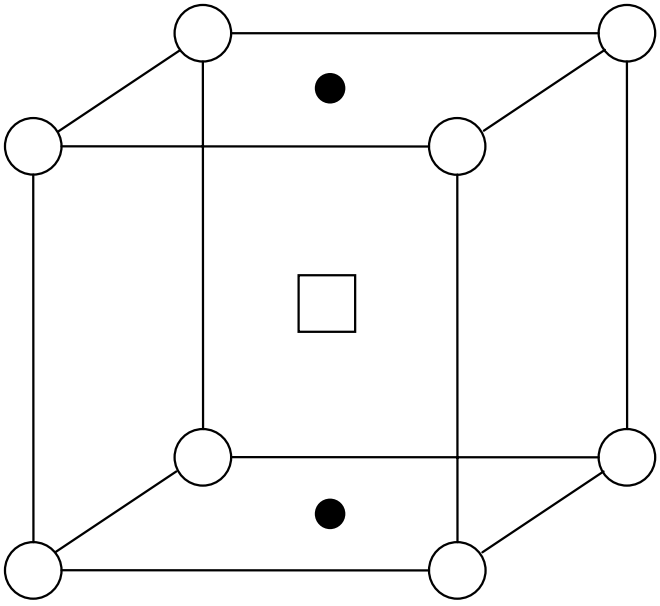

Fig. 5. The most stable configuration of a vacancy–two carbon binding in bcc Fe according to the present potential. The small black circles, large white circles and the square represent carbon, Fe atoms, and the vacancy, respectively.

0.12 eV. A CALPHAD [32,33] type thermodynamic assessment study of the Fe–C binary system is also available [29]. According to this study, the dilute heat of solution of carbon in bcc Fe is 1.11 eV, which is in good agreement with the experimental value, 1.1 eV [14]. The same quantity for fcc Fe according to this thermodynamic assessment study is 0.36 eV, which is also in good agreement with the present prediction. The relaxations of surrounding Fe atoms are small compared to those in bcc Fe, yielding 5.7% and 3.1% increases in the distance between carbon and the six first nearest Fe atoms along the ⟨1 0 0⟩ direction and between carbon and the eight second nearest Fe atoms along the ⟨1 1 1⟩ direction, respectively.

Table 4
Physical properties of the fcc Fe–C alloys calculated using the present 2NN MEAM potential, in comparison with experimental data or other calculations

In fcc Fe (eV)	MEAM	expt./calc.
Dilute heat of solution of carbon	0.30	0.36[a], 0.12[b]
Migration energy barrier of carbon	1.52	1.4[c], 1.53[d]
Vacancy–carbon binding energy	0.67	0.37–0.41[e]
Carbon–carbon binding energy	−0.12 ⟨1 1 0⟩ −0.35 ⟨1 0 0⟩	
Self interstitial–carbon binding energy	0.58	
Vacancy–two carbon binding energy	1.55 ⟨1 0 0⟩ 1.08 ⟨1 1 0⟩	

The crystallographic directions ⟨1 1 0⟩, etc., represents the direction of carbon–carbon alignment (see text). The reference states of all bindings are the states where all the individual defects are separated and non-interacting with each other.

[a] Thermodynamic assessment [29].
[b] First-principles calculation [28].
[c] Ref. [22].
[d] Ref. [34].
[e] Experiments and first-principles calculation [28].

Concerning the migration of interstitial carbon atoms in fcc Fe, it has been proposed [2] that passing the tetrahedral site, as is the case in bcc Fe, cannot be the migration path, because the migration energy is computed to be too high compared to the experimental value, 1.4–1.53 [22,34], along this path. The most favorable diffusion path for carbon atoms was proposed to be the ⟨1 1 0⟩ direction, and the saddle point to be half way between neighboring octahedral sites along the ⟨1 1 0⟩ direction [2]. Similar results were obtained with the present potential, and the migration energy barrier of carbon was calculated using the same method as in Ref. [2]. The present calculation predicts the migration energy of carbon in fcc Fe to be 1.52 eV, again in good agreement with the experimental value of 1.4–1.53 eV. As in the bcc solid solution, the carbon atom in the vacancy–carbon binding is not located close to the center of the vacancy, but is located almost exactly on the original octahedral site. The calculated binding energy is 0.67 eV, which is larger than the 0.37–0.41 eV proposed from experimental information and first-principles calculation [28].

In contrast to the bcc Fe–C solid solution, the carbon–carbon binding in neighboring octahedral sites is predicted to be energetically unfavorable. Two cases were considered (Fig. 6), one where two carbon atoms are located in the first nearest-neighboring interstitial sites being aligned along the ⟨1 1 0⟩ direction, and the other where two carbon atoms are located in the second nearest-neighboring interstitial sites aligned along the ⟨1 0 0⟩ direction with an Fe atom between them. According to the present potential, the binding energy for the first case (first nearest ⟨1 1 0⟩ alignment, Fig. 6(a)) is −0.12 eV, while that for the second case (second nearest ⟨1 0 0⟩ alignment, Fig. 6(b)) is −0.35 eV. It has been experimentally deduced that the repulsion between carbon atoms occupying neighboring interstitial sites is weak whereas carbon atoms as second nearest neighbors repulse each other strongly [20], which qualitatively supports the present calculations.

The binding energy between a self-interstitial and a carbon atom is also large in fcc Fe. In fcc metals, the most stable shape of a self-interstitial is a ⟨1 0 0⟩ dumbbell. The largest binding energy, 0.58 eV, is obtained when the interstitial carbon atom is located on the nearest-neighbor octahedral site from the center of a ⟨1 0 0⟩ dumbbell, perpendicular to the dumbbell direction. A strong binding between one vacancy and two carbon atoms is also predicted in fcc Fe. As in the case of bcc Fe, the most stable vacancy–two carbon binding configuration is a ⟨1 0 0⟩ carbon dumbbell with the vacancy at the center of the dumbbell. However, in contrast to the case in bcc Fe, the carbon atoms are not relaxed toward each other but remain on their original octahedral sites. The configuration where two carbon atoms align in a ⟨1 1 0⟩ direction on nearest-neighbor sites of the vacancy so that the carbon–vacancy–carbon bonding angle becomes 90° is also pre-

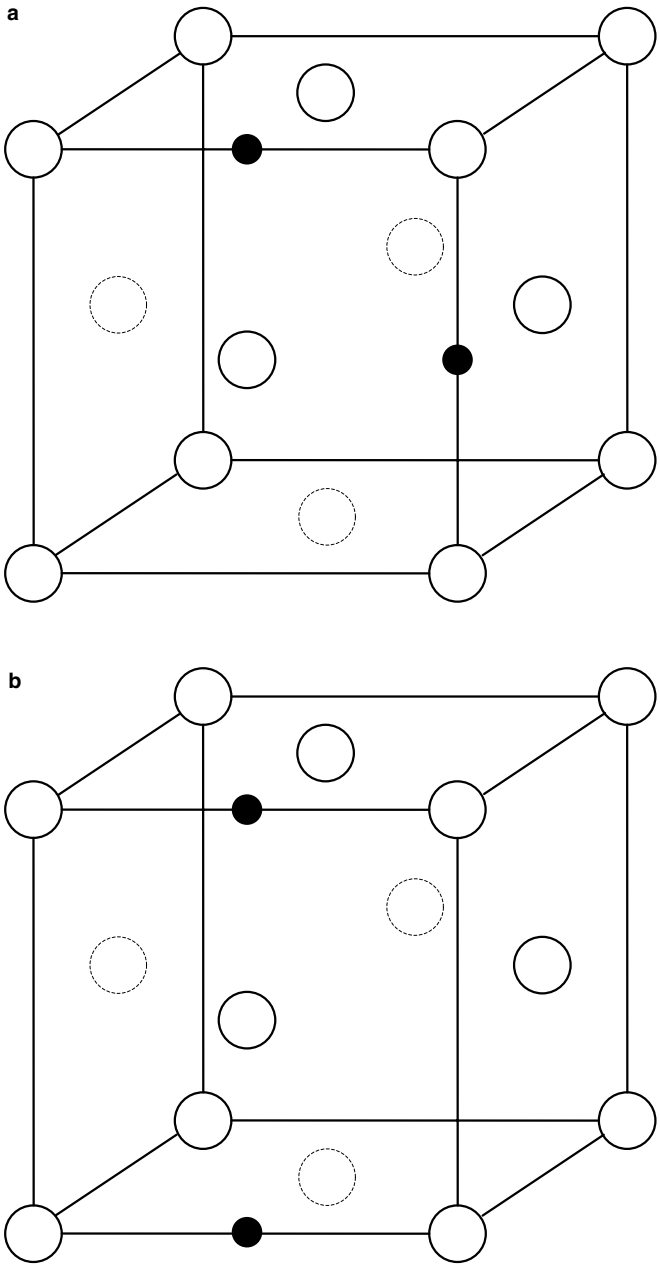

Fig. 6. Configurations of two carbon interstitial atoms in fcc Fe where two carbon atoms are located (a) in the first nearest-neighboring interstitial sites along the ⟨1 1 0⟩ direction, and (b) in the second nearest-neighboring interstitial sites along the ⟨1 0 0⟩ direction. The small black circles and large white circles represent carbon and Fe atoms, respectively.

dicted to be energetically favorable, but with less binding energy than the above ⟨1 0 0⟩ binding. It should be mentioned here that the present potential also predicts a positive binding between one vacancy and the six nearest-neighbor carbon atoms with a binding energy of 2.79 eV.

3.3. Carbides

It has been shown that the present MEAM potential reproduces very well the known physical properties of carbon as an interstitial solute element in bcc and fcc Fe, whether or not the individual properties were included during potential parameter optimization. The potential can be used reliably to investigate the interactions between carbon interstitial solute atoms and other defects such as vacancies, dislocations and grain boundaries. By correctly describing the relaxations of iron atoms around interstitial carbon atoms, this potential can also be used to investigate the effects of carbon on various deformation and mechanical behaviors of iron. However, investigating only the Fe–C binary behavior is not the final goal of this atomistic approach. It should be possible to investigate higher order alloy systems including more alloying elements using the same approaches. For this, the potential should be extended to higher order systems, involving many other elements with different equilibrium structures. As already mentioned, describing interatomic potentials of a wide range of elements using a common potential formalism and being able to deal with various alloy systems easily is the strongest point of the present (2NN) MEAM potential formalism. Naturally, the next step of the present study would be to extend the potential into many Fe–metal–C ternary systems. Fe–metal–C ternary systems are characterized by the formation of various carbides as well as the solution effects of the solute ''metal'' elements. Therefore, before proceeding to multi-component systems, it is important to further check the transferability and to learn the limits of the applicability of the present Fe–C potential, especially concerning the carbide phases.

As a means of checking the transferability of the present potential, the formation energies and lattice parameters of Fe_3C cementite and NaCl-type FeC were calculated. In the case of cementite, the calculation results could be compared with experimental information because the cementite is a real carbide. Though the NaCl-type FeC is not a real carbide in the Fe–C system, first-principles calculation results [24–26] are available for the cohesive energy, lattice parameter and bulk modulus. The results of these calculations are compared with the experimental or high-level calculation data in Table 5. The cementite is not a stable carbide in the Fe–C binary system. According to a thermodynamic assessment of the Fe–C system [29], the formation enthalpy of the cementite is about +0.06 eV for the reference states of bcc Fe and graphite carbon, at 298 K. The present MEAM potential predicts a value of +0.02 eV at 0 K. The lattice parameters are also comparable to the experimental data [30], even though these data were not considered during parameter optimization. However, it should be mentioned that some relaxations of atomic positions occurred during energy minimization, and small fluctuations in the atom positions and cohesive energy were observed even at 0 K. Further, the cementite structure could not be maintained during high-temperature MD (molecular dynamics) runs (above 600 K), yielding slightly transformed structures with more negative cohesive energies than the initial structure by about a few hundredths of an eV. This means that the present potential is not adequate to investigate in detail the stability, atomic struc-

Table 5
Physical properties of metastable carbides in the Fe–C system calculated using the present 2NN MEAM potential, in comparison with experimental data or other calculations

	MEAM	expt./calc.
Cementite		
Heat of formation (eV)	+0.02	+0.06[a]
Lattice constants, *a*, *b*, *c* (Å)	5.16, 6.32, 4.66	5.09, 6.74, 4.52[b]
NaCl-type FeC		
Cohesive energy (eV)	−5.36	−5.26[c]
Lattice constant, *a* (Å)	4.08	4.08[d]
Bulk modulus (GPa)	420	280[e]

[a] Thermodynamic assessment [29].
[b] Ref. [30].
[c] First-principles calculation [24].
[d] First-principles calculation [25].
[e] First-principles calculation [26].

ture and interface structure with matrix of cementite at non-zero temperatures (especially above the room temperature).

According to the present potential, the NaCl-type FeC structure was not stable, and various transformed structures resulted during MD runs at finite temperatures. The calculated values in Table 5 are those obtained just before the start of the collapse of the initial NaCl structure at 0 K. The calculated bulk modulus should be regarded as a rough estimation because a convergent cohesive energy value could not be obtained. Even though no special attention was paid to the lattice parameter of the FeC, the agreement with the first-principles calculation is quite good. However, it should be mentioned again that some of the transformed structures after the collapse of the NaCl-type structure were calculated to have larger cohesive energies than the average of those for pure Fe and carbon. Eventually, it was found that the most stable structure at 50 at.% C was the ZnS-type structure, with an erroneously negative formation energy of about −0.25 eV. Even though great efforts have been made to minimize the stability of this structure, the occurrence of this unanticipated stable structure could not be avoided. Therefore, care should be taken when using the present potential at high carbon content regions. One should check whether the initial matrix structure is kept or a different structure is created during high-temperature MD runs, although it would be impossible to observe the formation of ZnS-type FeC during normal MD simulation times.

Even with the limitations mentioned above, it is believed that the potential can be used to analyze the stability and interaction with the matrix of relatively simple MC and also hopefully M_2C-type carbides in Fe–metal–C ternary systems. As has already been shown, the stability and lattice parameter of hypothetical FeC is reasonably reproduced. The present author also already confirmed that the stability and lattice parameter of the same NaCl-type TiC carbide and the solute behavior of carbon in pure titanium could be correctly reproduced [35], using the present carbon potential [11] and a newly developed titanium potential [36]. Therefore, it should be possible to describe correctly the solute behavior of carbon and structural behavior of MC-type (Fe,Ti)C in the Fe–Ti–C ternary system. A promising result could also be obtained for the MC and M_2C-type carbides in the V–C binary system [35], using the already developed vanadium potential [9] and the carbon potential [11].

4. Conclusion

It has been shown that the present 2NN MEAM potential when applied to the Fe–C binary system can reproduce various physical properties such as the dilute heat of solution of carbon, the vacancy–carbon binding energy and its configuration, the location of interstitial carbon atoms and the migration energy of carbon atoms in bcc and fcc Fe, in good agreement with experimental information. In particular, the potential gives good agreement with fcc properties even though only bcc properties were used for fitting, which shows that the formalism is predictive. The potential can be used reliably to investigate the interactions between carbon interstitial solute atoms and other defects such as vacancies, dislocations and grain boundaries, and even to investigate the effects of carbon on various deformation and mechanical behaviors of iron. Some limitations are also expected when dealing with complex carbides using this semi-empirical interatomic potential in multi-component carbide systems. Even with these limitations, the potential can be easily extended to multi-component Fe–metal–C systems and used to analyze the stability and interaction with the matrix of relatively simple MC and M_2C-type carbides as well as the solution effects of solute "metal" elements.

Acknowledgments

This work was financially supported by the Ministry of Commerce, Industry and Energy of Korea through the core technology research program.

Appendix

One of the main differences between the MEAM and other empirical potentials is the use of many-body screening in the MEAM. The creation of the 2NN MEAM was also achieved by modifying the many-body screening so that it becomes less severe than in the original MEAM. Therefore, it would be worth describing once again the many-body screening [13] used in the MEAM formalism.

In the original MEAM [6], the neglect of the second nearest-neighbor interactions is effected by the use of a strong many-body screening function [13]. In the same way, the consideration of the second nearest-neighbor interactions in the modified formalism (2NN MEAM [8–10]) is effected by adjusting the many-body screening function so that it becomes less severe. In the MEAM, the many-body screening function between atoms *i* and *j*,

S_{ij}, is defined as the product of the screening factors, S_{ikj}, due to all other neighbor atoms k:

$$S_{ij} = \prod_{k \neq i,j} S_{ikj}. \tag{A.1}$$

The screening factor S_{ikj} is computed using a simple geometric construction. Imagine an ellipse on an x, y plane, passing through atoms i, k and j with the x-axis of the ellipse determined by atoms i and j. The equation of the ellipse is given by

$$x^2 + \frac{1}{C}y^2 = \left(\frac{1}{2}R_{ij}\right)^2. \tag{A.2}$$

For each k atom, the value of parameter C can be computed from relative distances among the three atoms, i, j and k, as follows:

$$C = \frac{2(X_{ik} + X_{kj}) - (X_{ik} - X_{kj})^2 - 1}{1 - (X_{ik} - X_{kj})^2}, \tag{A.3}$$

where $X_{ik} = (R_{ik}/R_{ij})^2$ and $X_{kj} = (R_{kj}/R_{ij})^2$. The screening factor S_{ikj} is defined as a function of C as follows:

$$S_{ikj} = f_c\left[\frac{C - C_{\min}}{C_{\max} - C_{\min}}\right], \tag{A.4}$$

where $C_{\min}$ and $C_{\max}$ are the limiting values of C determining the extent of screening and the smooth cutoff function is

$$\begin{array}{ll} f_c(x) = 1, & x \geqslant 1, \\ [1 - (1-x)^4]^2, & 0 < x < 1, \\ 0, & x \leqslant 0. \end{array} \tag{A.5}$$

The basic idea for the screening is that, first, two limiting values are defined, $C_{\max}$ and $C_{\min}$ ($C_{\max} > C_{\min}$). Then, if the atom k is outside of the ellipse defined by $C_{\max}$, it is thought that the atom k does not have any effect on the interaction between atoms i and j. If the atom k is inside of the ellipse defined by $C_{\min}$ it is thought that the atom k completely screens the i–j interaction, and between $C_{\max}$ and $C_{\min}$ the screening changes gradually. In the numerical procedure of simulation the electron density and pair potential are multiplied by the screening function S_{ij}. Therefore, $S_{ij} = 1$ and $S_{ij} = 0$ mean that the interaction between atoms i and j is unscreened and completely screened, respectively. In the original MEAM [6], $C_{\max} = 2.8$ and $C_{\min} = 2.0$ were chosen. These values ensure that for the fcc structure first nearest neighbors are completely unscreened for reasonably large thermal vibration, and the interactions are still first neighbor only even in the bcc structure. In addition to the many-body screening function, a radial cutoff function which is given by $f_c[(r_c - r)/\Delta r]$, where r_c is the cutoff distance and Δr (0.1 Å) is the cutoff region, is also applied to the atomic electron density and pair potential [13]. The radial cutoff distance is chosen so that it does not have any effect on the calculation results due to the many-body screening. This is only for computational convenience, that is, to save computation time.

References

[1] Johnson RA, Dienes GJ, Damask AC. Acta Metall 1964;12:1215.
[2] Rosato V. Acta Metall 1989;37:2759.
[3] Ruda M, Farkas D, Abriata J. Scripta Mater 2002;46:349.
[4] Daw MS, Baskes MI. Phys Rev Lett 1983;50:1285; Phys Rev B 1984;29:6443.
[5] Carlsson AE. In: Ehrenreich H, Turnbull D, editors. Solid state physics: advances in research and application, vol. 43. New York (NY): Academic Press; 1990.
[6] Baskes MI. Phys Rev B 1992;46:2727.
[7] Foiles SM, Baskes MI, Daw MS. Phys Rev B 1986;33:7983.
[8] Lee B-J, Baskes MI. Phys Rev B 2000;62:8564.
[9] Lee B-J, Baskes MI, Kim H, Cho YK. Phys Rev B 2001;64:184102.
[10] Lee B-J, Shim J-H, Baskes MI. Phys Rev B 2003;68:144112.
[11] Lee B-J, Lee JW. CALPHAD 2005;29:7.
[12] Rose JH, Smith JR, Guinea F, Ferrante J. Phys Rev B 1984;29:2963.
[13] Baskes MI. Mater Chem Phys 1997;50:152.
[14] Hultgren R, Desai PD, Hawkins DT, Gleiser M, Kelley KK. Selected values of the thermodynamic properties of binary alloys. Metals Park (OH): ASM; 1973.
[15] Arndt RA, Damask AC. Acta Metall 1964;12:341.
[16] Weller M, Diehl J. Scripta Metall 1976;10:101.
[17] Vehanen A, Hautojärvi P, Johansson J, Yli-Kauppila J, Moser P. Phys Rev B 1982;25:762.
[18] Takaki S, Fuss J, Kugler H, Dedek U, Schults H. Radiat Eff 1983;79:87.
[19] Hautojärvi P, Johansson J, Vehanen A, Yli-Kauppila J, Moser P. Phys Rev Lett 1980;44:1326.
[20] Gavriljuk VG, Berns H. High nitrogen steels: structure, properties, manufacture, applications. Berlin: Springer-Verlag; 1999.
[21] Williamson GK, Smallmann RE. Acta Crystallogr 1953;6:361.
[22] Askill J. Tracer diffusion data for metals, alloys and simple oxides. New York (NY): Plenum Press; 1970.
[23] Le Claire AD. In: Mehrer H, editor. Numerical data and functional relationships in science and technology. Landolt-Börnstein, New Series, Group III, vol. 26. Berlin: Springer-Verlag; 1990. p. 480–1.
[24] Fernández Guillermet A, Grimvall G. J Phys Chem Solids 1992;53:105.
[25] Häglund J, Grimvall G, Jarlborg T, Fernández Guillermet A. Phys Rev B 1991;43:14400.
[26] Häglund J, Fernández Guillermet A, Grimvall G, Körling M. Phys Rev B 1993;48:11685.
[27] Domain C, Becquart CS, Foct J. Phys Rev B 2004;69:144112.
[28] Slane JA, Wolverton C, Gibala R. Metall Mater Trans A 2004;35:2239.
[29] Gustafson P. Scand J Metallurgy 1985;14:259.
[30] Villars P, Calvert LD. Pearson's handbook of crystallographic data for intermetallic phases. second ed. Materials Park (OH): ASM International; 1991.
[31] Johnson RA, Damask AC. Acta Metall 1964;12:443.
[32] Kaufman L, Bernstein H. Computer calculation of phase diagrams. New York (NY): Academic Press; 1970.
[33] Saunders N, Miodownik AP. CALPHAD: a comprehensive guide. Pergamon materials series, vol. 1. New York: Pergamon Press; 1998.
[34] Brandes EA, Brook GB, editors. Smithells metals reference book. Oxford: Butterworth-Heinemann; 1992.
[35] Lee B-J. Pohang University of Science and Technology, Korea, unpublished work; 2004.
[36] Kim YM, Lee B-J. Pohang University of Science and Technology, Korea, unpublished work; 2004.